Comparison of Ca^{2+} Sparks Produced Independently by Two Ryanodine Receptor Isoforms (Type 1 or Type 3)

Matthew W. Conklin,* Chris A. Ahern,* Paola Vallejo,* Vincenzo Sorrentino,†‡ Hiroshi Takeshima,§ and Roberto Coronado*

*Department of Physiology, University of Wisconsin, Madison, Wisconsin 53706 USA; †DIBIT San Raffaele Scientific Institute, Milan, Italy; ‡Dipartimento di Scienze Biomediche, Università degli Studi di Siena, Siena, Italy; and §Department of Pharmacology, Faculty of Medicine, University of Tokyo, Tokyo 113, Japan

ABSTRACT The molecular determinants of a Ca^{2+} spark, those events that determine the sudden opening and closing of a small number of ryanodine receptor (RyR) channels limiting Ca^{2+} release to a few milliseconds, are unknown. As a first step we investigated which of two RyR isoforms present in mammalian embryonic skeletal muscle, RyR type 1(RyR-1) or RyR type 3 (RyR-3) has the ability to generate Ca^{2+} sparks. Their separate contributions were investigated in intercostal muscle cells of RyR-1 null and RyR-3 null mouse embryos. A comparison of Ca^{2+} spark parameters of RyR-1 null versus RyR-3 null cells measured at rest with fluo-3 showed that neither the peak fluorescence intensity ($\Delta F/F_o = 1.25 \pm 0.7$ vs. 1.55 ± 0.6), spatial width at half-max intensity (FWHM $= 2.7 \pm 1.2$ vs. 2.6 ± 0.6 μm), nor the duration at half-max intensity (FTHM $= 45 \pm 49$ vs. 43 ± 25 ms) was significantly different. Sensitivity to caffeine (0.1 mM) was remarkably different, with sparks in RyR-1 null myotubes becoming brighter and longer in duration, whereas those in RyR-3 null cells remained unchanged. Controls performed in double RyR-1/RyR-3 null cells obtained by mice breeding showed that sparks were not observed in the absence of both isoforms in >150 cells imaged. In conclusion, 1) RyR-1 and RyR-3 appear to be the only intracellular Ca^{2+} channels that participate in Ca^{2+} spark activity in embryonic skeletal muscle; 2) except in their responsiveness to caffeine, both isoforms have the ability to produce Ca^{2+} sparks with nearly identical properties, so it is rather unlikely that a single RyR isoform, when others are also present, would be responsible for Ca^{2+} sparks; and 3) because RyR-1 null cells are excitation-contraction (EC) uncoupled and RyR-3 null cells exhibit a normal phenotype, Ca^{2+} sparks result from the inherent activity of small clusters of RyRs regardless of the participation of these RyRs in EC coupling.

INTRODUCTION

Three ryanodine receptor (RyR) isoforms have been described in various mammalian tissues (Takeshima et al., 1989; Nakai et al., 1990; Hakamata et al., 1992) and related variants in avian and amphibian tissues (Sutko and Airey, 1996). The three mammalian RyRs share a high sequence identity (>65%), although key differences have been noticed and these may be related to tissue-specific functions. In muscle, RyR type 1 (RyR-1) is predominantly expressed in adult skeletal muscles, RyR type 2 (RyR-2) is the major adult cardiac isoform, and RyR type 3 (RyR-3) is present in smooth muscle and in embryonic striated muscle (Sorrentino and Reggiani, 1999). RyR types 1 and 2 play a central role in voltage-dependent activation of Ca^{2+} release in their respective tissues during excitation-contraction (EC) coupling (Coronado et al., 1994). Both isoforms interact closely with the dihydropyridine receptor (DHPR) and colocalize with DHPRs in junctions formed by the sarcoplasmic reticulum (SR) and t-system membranes (Block et al., 1988; Carl et al., 1995).

The contribution of RyR types 1 and 3 to EC coupling in skeletal muscle was addressed using RyR-1 or RyR-3 knockout mice (Takeshima et al., 1994, 1996; Bertocchini et al., 1997; Barone et al., 1998). Absence of RyR-1 leads to loss of EC coupling function, paralysis of skeletal muscles, and absence of postnatal survival (Takeshima et al., 1994; Nakai et al., 1996). The EC coupling function is unique to RyR-1 because neither RyR-2 nor RyR-3 supports skeletal-type EC coupling when expressed in RyR-1-deficient skeletal muscle cells (Nakai et al., 1997; Ward et al., 1999). Absence of RyR-3 affects some dynamic aspects of embryonic muscle tension but is not essential for mouse survival (Takeshima et al., 1996; Bertocchini et al., 1997). There are additional differences in sensitivity to cytosolic ligands that set RyR-1 and RyR-3 apart. Avian skeletal muscle is endowed with α and β RyR isoforms, of which β was shown to be homologous to mammalian RyR-3 (Ottini et al., 1996). Under the same ligand conditions, 60% of the openings of chick RyR type β channels are ~50-fold longer than the bulk of the openings of chick RyR type α channels (Percival et al., 1994). Also, type β channels remain open over a wider range of cytoplasmic Ca^{2+} and, in the presence of ATP, are not inactivated by Ca^{2+} (Percival et al., 1994). A long mean open time has also been reported in the mammalian RyR-3 channel (Chen et al., 1997). This result and the low sensitivity of mammalian RyR-3 to inactivation by Ca^{2+} (Sonnleitner et al., 1998) and by Mg^{2+} (Murayama and Ogawa, 1997) suggest that RyR-3 channels in situ could

Received for publication 22 October 1999 and in final form 11 January 2000.

Address reprint requests to Roberto Coronado, Dept. of Physiology, University of Wisconsin, 1300 University Ave., Madison, WI 53706. Tel.: 608-263-7487; Fax: 608-265-5512; E-mail: coronado@physiology.wisc.edu.

0006-3495/00/04/1777/09 $2.00

remain open for considerably longer periods than RyR-1 channels.

In heart and skeletal muscle the spontaneous activity of RyR channels in cells at rest results in Ca^{2+} sparks with highly stereotypic properties (Cheng et al., 1993; Klein et al., 1996; Conklin et al., 1999a). The RyR isoforms directly responsible for these spark activities are unknown. RyR types α and β in amphibian skeletal muscle and RyR-2 in mammalian ventricle are highly likely to engage in sparks because 1) sparks were originally reported in these adult tissues (Cheng et al., 1993; Tsugorka et al., 1995) and 2) so far, these are the only isoforms reported in these adult tissues. However, sparks were not observed in the adult rat EDL muscle (Shirokova et al., 1998) although they were clearly seen, albeit at a low frequency, in the adult mouse FDB muscle (Conklin et al., 1999b). Thus, whether mammalian RyR-1 or RyR-3 engages in stereotypic Ca^{2+} spark activity remains to be thoroughly elucidated.

We previously showed that RyR-3 augments the dimensions of spontaneously occurring Ca^{2+} sparks in embryonic mouse skeletal muscle cells (Conklin et al., 1999b). However, this study could not resolve whether RyR-3 by itself in the absence of RyR-1 could produce Ca^{2+} sparks. In the present study we used RyR-1 null myotubes, which are known to express RyR-3 (Takeshima et al., 1995), and RyR-3 null myotubes, which are functionally normal and are known to express RyR-1 (Takeshima et al., 1996) to test the separate contributions of RyR-3 and RyR-1 to Ca^{2+} sparks in embryonic skeletal muscle. As controls, we used double RyR knockout types 1 and 3 null myotubes. Spontaneous Ca^{2+} sparks were not detectable when both RyRs were knocked out. The Ca^{2+} spark parameters suggested that RyR-3 has the same ability as RyR-1 to generate these miniature Ca^{2+} release events. Part of these results were previously published in abstract form (Conklin et al., 1999c).

MATERIALS AND METHODS

RyR-1 null and RyR-3 null mice

Screening of the RyR-1 and RyR-3 wild-type (wt) and null alleles was done respectively by PCR and Southern blot analysis using established protocols (Takeshima et al., 1994; Bertocchini et al., 1997). Double-null embryos were obtained by breeding mice heterozygous for the RyR-1 null allele (RyR-$1^{+/-}$) and homozygous for the RyR-3 null allele (RyR-$3^{-/-}$).

Single cell preparations

Embryonic myotubes were enzymatically dissociated from intercostal muscles of embryonic day 18 (E18) RyR-1 null, RyR-3 null, and RyR types 1 and 3 double-null mice as described (Conklin et al., 1999b). Isolated cells were allowed to settle in a culture dish with the bottom replaced by a thin glass coverslip for at least 1 h before imaging. Embryonic cells were viable for several hours, as demonstrated by their ability to maintain a relatively constant low resting fluo-3 fluorescence and absence of Di-8-ANEPPS penetration into the cytosol. The total number of cells from which sparks were collected was 67 cells from 12 RyR-1 null embryos and 66 cells from 30 RyR-3 null embryos. No sparks were seen in >150 cells imaged from 10 RyR types 1 and 3 double-null embryos.

Ca^{2+} spark measurements

T-system and Ca^{2+} imaging was performed as described (Conklin et al., 1999b). Cells were allowed to settle at room temperature in Krebs buffer plus 2 mM $CaCl_2$ and stained with 17 μM Di-8-ANEPPS (Molecular Probes, Eugene, OR) for up to 10 min, followed by dye washout. Alternatively, cells were loaded with 4 μM fluo-3 acetoxymethyl (AM) ester (Molecular Probes) for up to 20 min. Cells were viewed with an inverted microscope with a 40× oil immersion objective (N.A. = 1.3) and a Fluoview (Olympus, Melville, NY) confocal attachment. The 488-nm spectrum line provided by a 5 mW argon laser attenuated to 6% was used for excitation of fluo-3 and Di-8-ANEPPS. The pixel size was 0.1–0.3 μm and the line-scan rate was 2.05 ms per 512-pixel line. Two-dimensional (2-D) images of Di-8-ANEPPS fluorescence were Kalman-averaged three times. Stock solutions of fluo-3 AM and Di-8-ANEPPS were prepared in DMSO.

RESULTS

The top images of Fig. 1 show intercostal muscle cells from RyR-1 null, RyR-3 null, and double type 1/type 3 null embryos loaded with fluo-3 AM in Krebs solution containing 2 mM Ca^{2+} at room temperature. All cells were capable of maintaining a low average cytosolic fluorescence for several hours, although sites of persistent elevated Ca^{2+} were clearly present in some cases. Ca^{2+} sparks were identified during repetitive scans performed at a fast speed and low laser intensity to avoid photobleaching. On average, ~25% of the RyR-1 null or RyR-3 null cells produced Ca^{2+} sparks and typically, these cells had several simultaneously active sites. Single sparks can be seen in the images of RyR-1 null and RyR-3 null cells, and the small insets show the same location in the cell without the spark. In double-null cells we failed to identify sparks in >150 cells repetitively scanned for several minutes in each case. The inset in the latter image shows that exposure of a double-null cell to 1 μM thapsigargin resulted in a large elevation in cytosolic Ca^{2+}. This result demonstrated that the inability of the double-null cell to generate sparks was not due to a generalized incapacity of these cells to store Ca^{2+} in the SR. We also used the cell-impermeant dye Di-8-ANEPPS to verify the integrity of the cell membrane and transverse tubular system (Shacklock et al., 1995) in the three cell types investigated. The bottom images of Fig. 1 shows that Di-8-ANEPPS fluorescence accumulated on the cell surface and in areas immediately adjacent to the cell surface. Some features of the nascent t-system, such as faint threads, were seen in all cells and are consistent with the longitudinal disposition of transverse tubules in mouse embryonic muscle seen in EM images (Franzini-Armstrong, 1991).

Fig. 2 shows line-scan images of Ca^{2+} sparks in each of the two RyR null cells. Time increases from left to right and only the region covered by the spark is shown in the image.

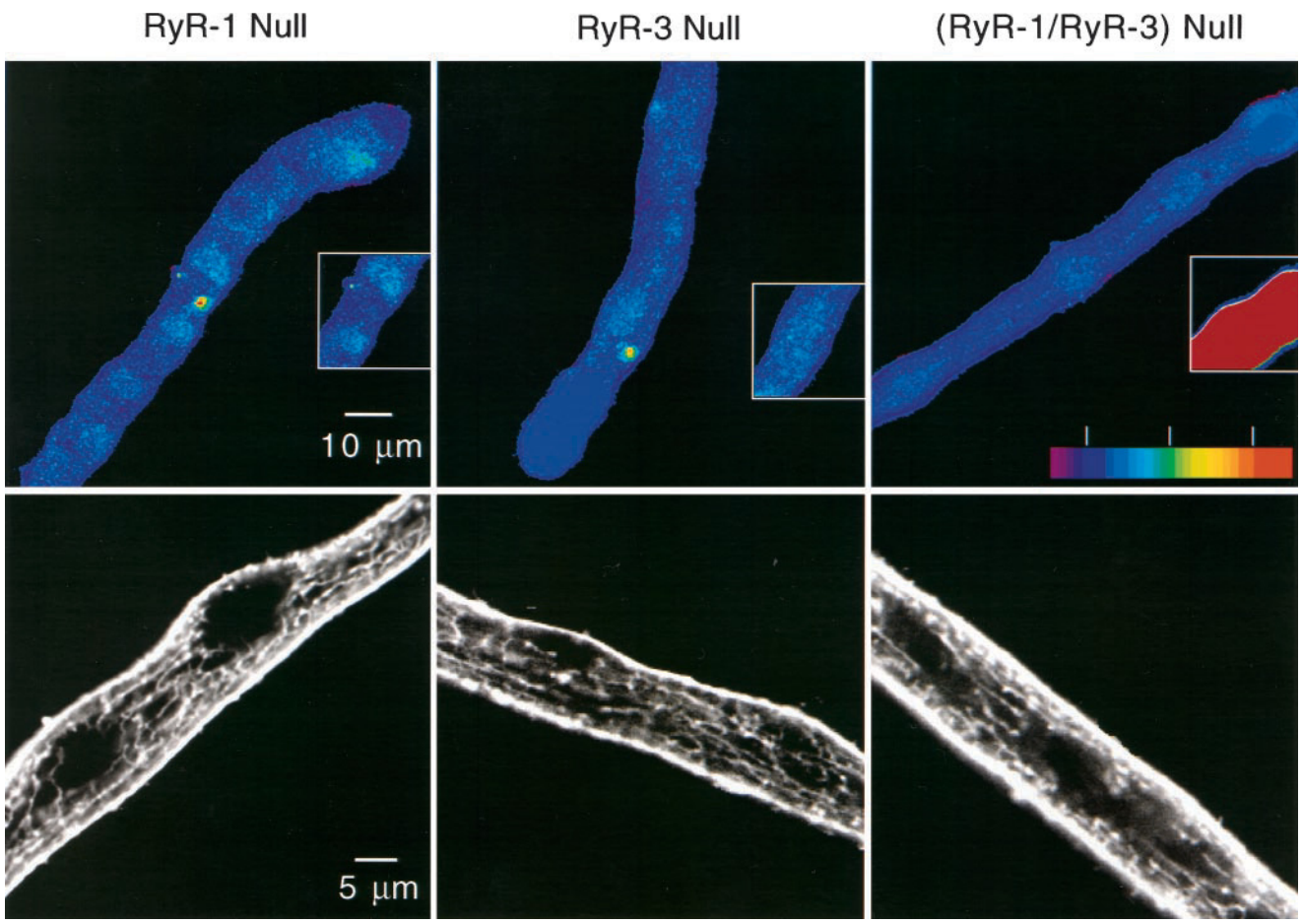

FIGURE 1 Top panels show confocal pseudocolor images of cells loaded with fluo-3 during a Ca^{2+} spark. Full-size images have a size of 512 × 512 pixels (0.2 × 0.2 μm per pixel) and were acquired at a rate of 1.2 s per image. Insets show the same area of the cell without the spark. An 8-pixel smoothing and a 32-color table were applied to highlight the location of the Ca^{2+} spark. Blue and red colors depict lower and higher fluorescence intensities, respectively. $\Delta F/F_o$ = 0, 1, and 2 are indicated. The 5-μm scale bar is the same for the three top images. Bottom panels show confocal gray-scale images of embryonic cells stained with 17 μM Di-8-ANEPPS.

Ca^{2+} sparks occurred repetitively at the same location, although the overall density of sparks was low in both cases. The overall rate of spark occurrence at sites engaged in the formation of sparks was ~1.9 sparks/scan (417 events captured in 221 scans) for RyR-3 null cells and ~1.6 sparks/scan (341 events captured in 208 scans) for RyR-1 null cells. In both cases, scans had a duration of 2.05 s. Considering the duration of the line-scan and the size of the cell, the spark frequencies were ~0.03 events/s/μm for both cell types. This frequency of spark occurrence represents a small fraction of that reported for depolarized cells, but it is close to that reported for frog skeletal muscle at rest (Klein et al., 1996). Inspection of the traces of the time course of fluorescence through the center of sites of sparks (Fig. 2, *bottom*) revealed a remarkable similarity between events in RyR-1 null and RyR-3 null cells. The spark onset was fast in both cell types and the peak amplitude and decay phases were also similar. In RyR-3 null cells there was a tendency for sparks to occur in rapid succession at the same site. These tandems were also noticed previously in normal cells (Conklin et al., 1999a) but were not observed in RyR-1 null cells.

Histograms of the half-width (FWHM), the maximum fluorescence intensity ($\Delta F/F_o$) and the half-duration (FTHM) of individual sparks collected in RyR-1 null (341 events from 67 cells) and RyR-3 null (412 events from 66 cells) cells are shown in Fig. 3. Sparks occurring in rapid succession for which the fluorescence did not decay to the baseline between events were excluded from these distributions. The frequency distributions of the three spark parameters were similar, consistent with the visual inspection of the line-scan data. The distributions were roughly symmetrical in the case of the half-width and asymmetric in the case of the peak intensity and half-duration. However, in neither case were these distributions bimodal. The distributions of half-durations were skewed, with a mean longer than the mode. Thus, brief events were overrepresented in both cases. A better appreciation of the kinetics of the spark was

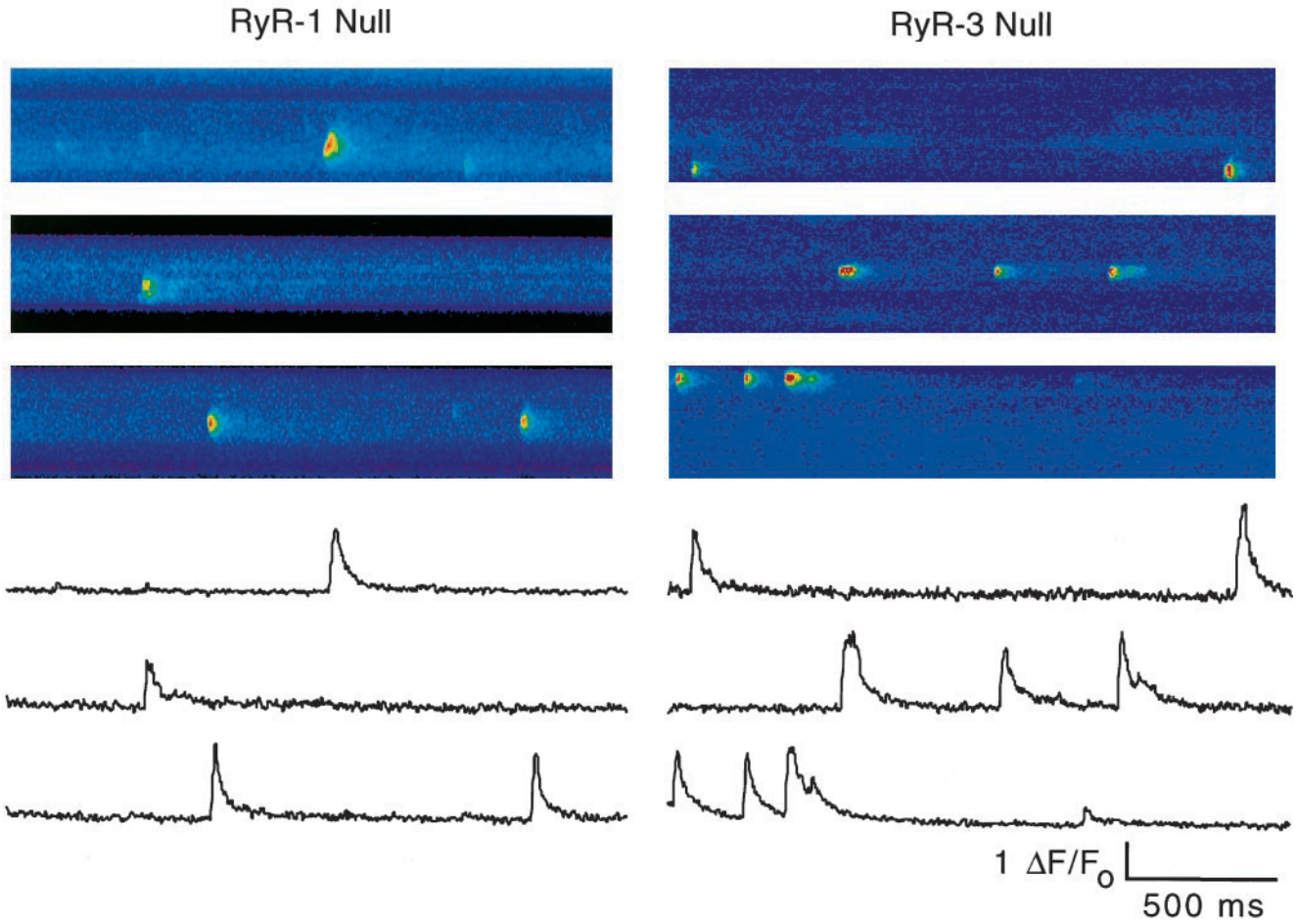

FIGURE 2 Ca^{2+} sparks in embryonic myotubes. The *top* shows confocal line-scan images of fluo-3 fluorescence from sparks each in a separate cell. Images have a size of 20 μm (*vertical*) $\times$ 2.05 s (*horizontal*) and a pixel size of 0.2 μm $\times$ 2.05 ms. The *bottom* shows the time course of the change in fluorescence intensity during a spark obtained by integration of the line-scan fluorescence of the images above.

obtained by plotting the three parameters of a single spark, namely FWHM, FTHM, and $\Delta F/F_o$, in three dimensions. These are shown at the bottom of Fig. 3. Three-dimensional (3-D) plots showed that there was a broad tendency for sparks to vary in intensity more than in dimension and duration. Accordingly, the shape of the 3-D distributions was roughly that of a vertical ellipsoid extending upward in the intensity (z) axis. In RyR-1 null cells there was a significant number of long-lasting sparks (FTHM $>$ 100 ms, $n = 36$ events) clearly not present in RyR-3 null cells. This group of sparks also had a higher half-width and a higher peak fluorescence, and produced a scattering of the 3-D distribution toward the top and the back of the 3-D plot. This observation is consistent with recordings of the RyR-3 avian homolog channel, RyR type β, in planar bilayers. Under the same ligand conditions, 60% of the openings of chick β-RyR channels are ~50-fold longer than the bulk of the openings of chick α-RyR channels (Percival et al., 1994). Notwithstanding the group of large sparks in RyR-1 null cells, the overriding conclusion when the data is taken as a whole is that the specific absence of the RyR-1 or RyR-3 isoform in each of the null cell types did not affect the spatial and temporal properties of the bulk of the Ca^{2+} sparks produced by the remaining RyR isoform.

We further established that sparks were mediated by RyRs by treating cells with caffeine. *Panel A* of Fig. 4 shows line-scans in cells during a control period and ~5 min after the addition of 0.1 mM caffeine to the bath solution. In RyR-1 null cells Ca^{2+} sparks were prolonged and, in some cases, the frequency of events was also increased. In RyR-3 null cells this caffeine concentration produced no significant effect. This result is consistent with previous observations (Bertocchini et al., 1997) showing that RyR-3 null cells are remarkably insensitive to caffeine. Several sparks from the same site were averaged before and after exposure to caffeine and are shown in *panel A* as cropped line-scans. The time course of fluorescence change through the center of the spark average is shown in *panel B*. In RyR-1 null cells there was a significant prolongation of the spark duration, but the peak fluorescence remained

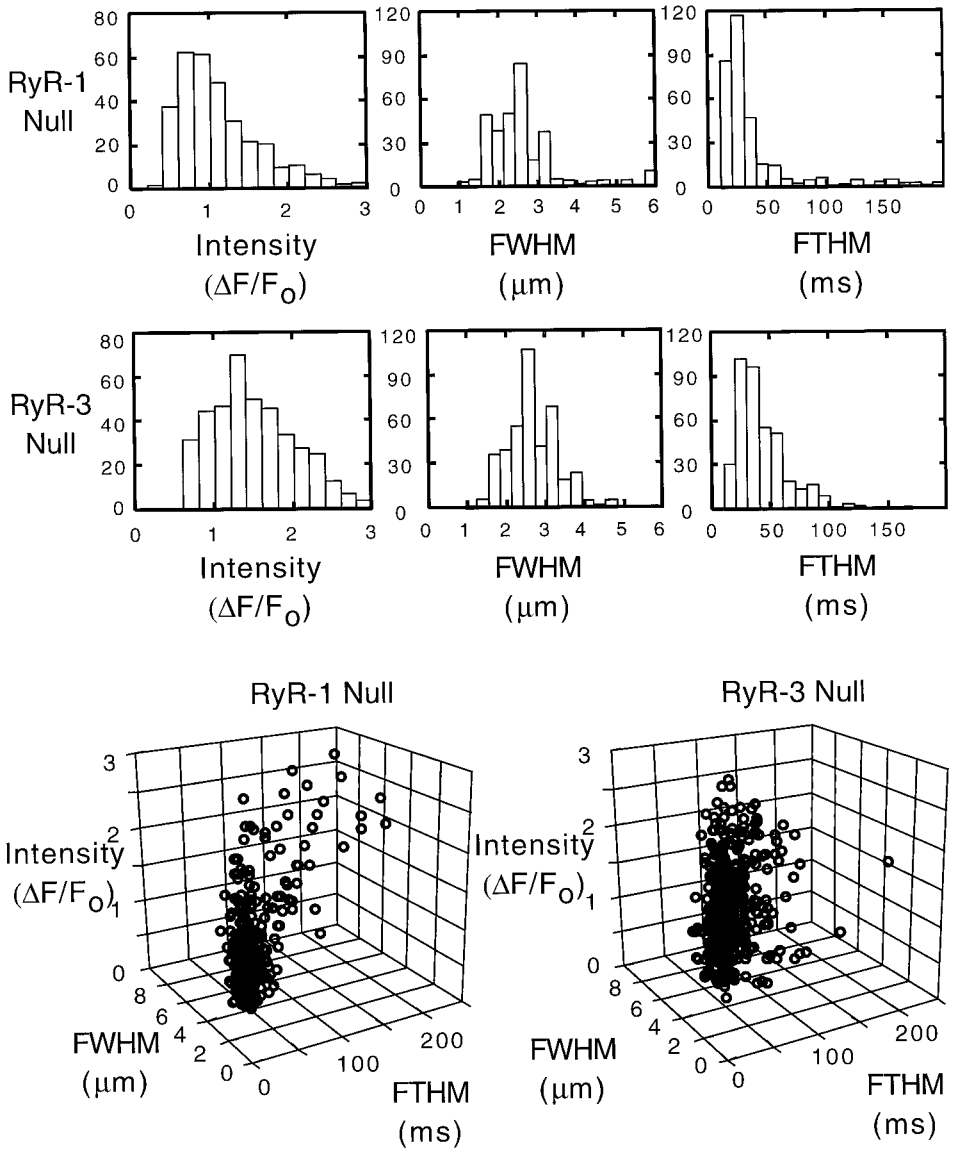

FIGURE 3 Histograms of spark parameters and relationship of Ca^{2+} spark width to intensity and duration. The peak fluorescence intensity in $\Delta F/F_o$ units, full-width at half-maximal fluorescence intensity (FWHM), and full-duration at half-maximal fluorescence intensity (FTHM), of sparks identified in RyR-1 null cells (341 events) and RyR-3 null cells (412 events). Plotted in three dimensions are the FTHM (x axis), FWHM (y axis), and $\Delta F/F_o$ (z axis) of each spark.

unchanged. Averaged for three sites, the fold-change of the Ca^{2+} spark parameters produced by 0.1 mM caffeine in RyR-1 null cells vs. RyR-3 cells were $+1.09 \pm 0.07$ vs. -1.03 ± 0.03 for the change in $\Delta F/F_o$, $+1.91 \pm 0.24$ vs. -1.01 ± 0.03 for the change in FTHM, and $+1.17 \pm 0.11$ vs. -1.09 ± 0.01 for the change in FWHM (mean $\pm$ SE; + or − denote increase or decrease, respectively; 1.0-fold denotes no change). We also attempted to measure the response of cells to a higher caffeine concentration. *Panel C* of Fig. 4 shows compressed line-scan images in cells exposed to 1 mM caffeine. In the millimolar range, caffeine produced a large increase in background fluorescence in RyR-1 null cells or a moderate increase in RyR-3 null cells that in both cases was incompatible with spark measurements. However, this high caffeine concentration had no effect on the resting fluorescence of double-null cells. The main conclusion from these experiments was that RyR-3 channels were significantly more sensitive to caffeine than RyR-1 channels and, furthermore, all the Ca^{2+}-mobilizing activity appeared to be mediated by these two RyR isoforms.

DISCUSSION

A first step toward understanding Ca^{2+} sparks in molecular terms is to establish which RyR isoform is capable of

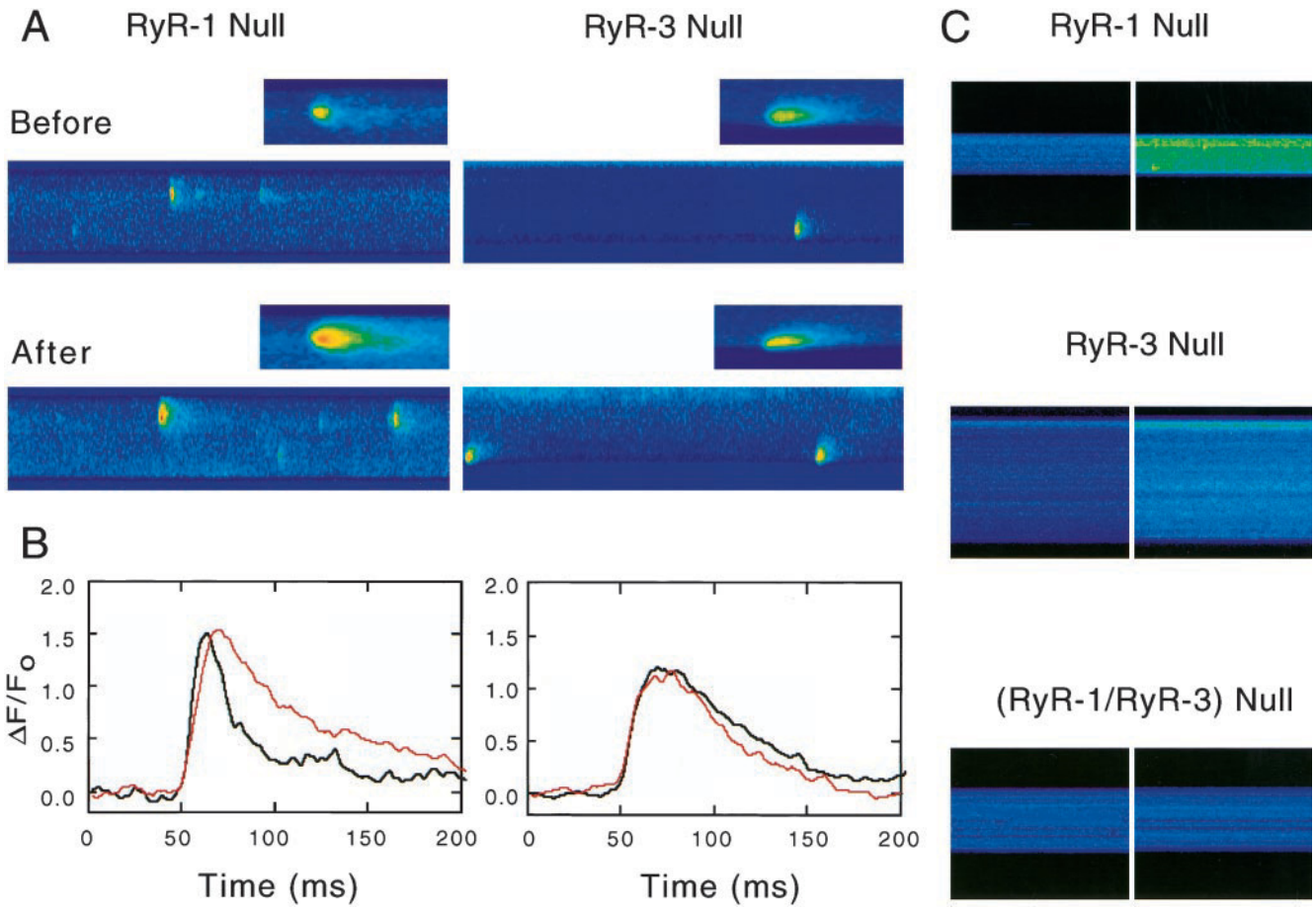

FIGURE 4 Stimulation of Ca^{2+} sparks by caffeine. *Panel A* shows line-scan images (15 μm vertical and 2.05 s horizontal) of sparks before and 5 min after the addition of caffeine at a final bath concentration of 0.1 mM. The cropped line-scans (7 μm $\times$ 205 ms) shown as insets are images of the same site obtained by averaging 5 sparks before and 8 sparks after in the RyR-1 null cell, and 8 sparks before and 6 sparks after in the RyR-3 null cell. *Panel B* shows the time course of the integrated fluorescence intensity of the average spark images above. *Panel C* shows line-scan images of the increase in cytosolic Ca^{2+} produced by a high caffeine concentration (1 mM). The two line-scan images for each cell type are before (*left*) and after (*right*) 1 mM caffeine. Image size is 60 μm (*vertical*) and 2.05 s (*horizontal*) in all cases.

generating Ca^{2+} sparks. We previously showed that RyR-1 in the absence of RyR-3 engages in Ca^{2+} spark activity in embryonic intercostal muscle cells (Conklin et al., 1999b). The present data further demonstrated that RyR-3 in the absence of RyR-1 also engages in Ca^{2+} spark activity. Hence both isoforms have an inherent ability to engage in Ca^{2+} spark activity. Moreover, inspection of double knockout cells led us to conclude that the two RyRs in question were the only intracellular channels that produced the sparks. Intracellular Ca^{2+} release channels formed by the inositol trisphosphate receptor could have contributed to the events measured here, given their ability to generate a multitude of miniature local Ca^{2+} transients in amphibian oocytes (Yao et al., 1995). Moreover, it could be argued that spark-producing inositol trisphosphate receptors were down-regulated in the double-null muscle cell due to an unforeseen pleiotropic effect. The contributions of inositol trisphosphate receptors to the present results was deemed highly unlikely, because "spark"-like activities produced by inositol trisphosphate receptors are much more heterogeneous than those encountered here. Also, sparks in each of the two RyR null cells were found to be inhibited by ryanodine (not shown) and inositol trisphosphate receptors have not been convincingly shown to be expressed in skeletal muscle.

Not only did each RyR subtype produce sparks, but a detailed comparison of the kinetics of the sparks showed events produced by RyR-1 or RyR-3 were indistinguishable. These observations are significant for two reasons. First, RyR-1 and RyR-3 have fundamentally different roles, as RyR-3 channels are not activated by voltage and do not support EC coupling. Our results suggest that resting Ca^{2+} sparks result from an inherent activity of RyRs unrelated to EC coupling. Specific roles of Ca^{2+} sparks in embryonic muscle unrelated to the EC coupling function were previously discussed (Conklin et al., 1999b). Second, the density

of RyR-3 in adult skeletal muscle is low (Jeyakumar et al., 1998), yet RyR-3 colocalizes with RyR-1 at junctional triads forming clusters in which both isoforms are present (Flucher et al., 1999). Our results suggest that in these clusters of RyR-1 channels essentially "doped" with RyR-3 channels, the impact of RyR-3 could be significant. An initial opening of an RyR-3 channel could activate RyR-1 channels present at a much higher density in the immediate surroundings of the activated RyR-3 channel. Hence, a single RyR-3 channel need only act as a trigger of a spark, while additional RyR-1 channels could quickly amplify the trigger Ca^{2+} to produce a full spark.

Additional inferences concerning clusters of RyRs can be brought about by comparing Ca^{2+} sparks in wt and RyR null cells. Table 1 summarizes the parameters of Ca^{2+} sparks reported previously in wt cells of the same age using the same microscope and imaging techniques (Conklin et al., 1999b) and those reported here for RyR-1 null and RyR-3 null cells. Sparks in wt cells lasted longer and were wider than in any of the two null cells. Also, sparks in wt muscle were brighter than those produced by RyR-3 in RyR-1 null cells. The single channel conductance is similar for RyR-1 and RyR-3 channels (Percival et al., 1994; Chen et al., 1997; Sonnleitner et al., 1998). Therefore, there are two explanations to consider for the difference in spark size and duration between the wt and RyR null muscle. Either the opening probability of RyR channels is higher in the wt cell or, alternatively, more RyRs were open during a spark in a wt cell than in each of the two mutant cells. The former possibility was considered unlikely because the overall frequency of sparks was considerably lower in wt cells, given the number of cells and the number of sparks collected from these cells (Table 1). In the context of the latter possibility, we suggest Ca^{2+} sparks could arise from densely packed clusters of RyRs such as those depicted in Fig. 5. Large clusters of RyRs, of the size depicted for E18 wt cells or larger, have been reported in primary myotubes cultured from embryonic muscle (Takekura et al., 1994). As indicated in Fig. 5, the specific absence of RyR-1 would lead to clusters composed exclusively of RyR-3. Briefer sparks in RyR-1 null cells could result from the fact that the density of RyR-3 is sparse, hence the probability of activating near-neighbor RyRs is reduced. It is also possible that these dilute clusters of RyR-3 channels could condense into small clusters of highly packed RyRs. Again, the expectation would be that sparks should be briefer and smaller because the size of the cluster is reduced. However, the specific absence of RyR-3 would lead to clusters of RyR-1 channels with defects in the packing lattice. These defects could be severe to the point that the activation of near-neighbor RyRs is compromised. It may also be possible that RyRs within this defective lattice could repack into smaller clusters. In either case, the parameters of sparks would be reduced.

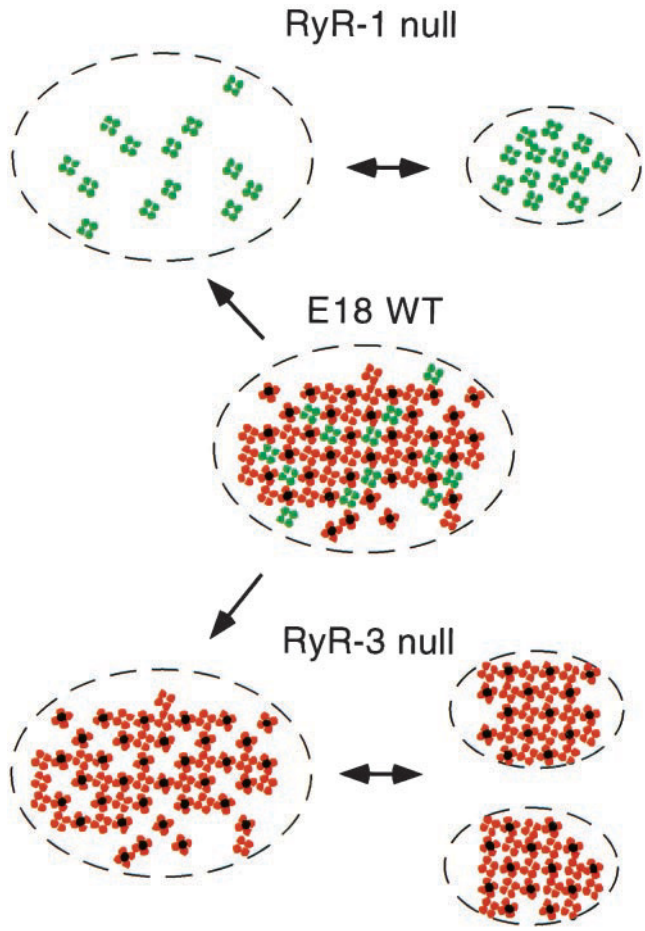

FIGURE 5 Models of RyR clustering in embryonic muscle. The center diagram shows a cluster of RyR-1 (*red*) and RyR-3 (*green*) arranged in a conventional side-to-side disposition described in myotubes in cell culture (Takekura et al., 1994). Dotted RyRs represent EC-coupled RyRs. According to the tetrad size (26 nm on its side), the cluster is ~0.3 μm wide. RyR-3 in RyR-1 null muscle (*top*) and RyR-1 in RyR-3 null muscle (*bottom*) may be present as dispersed RyRs or in high-density clusters smaller than those present in wt embryonic muscle.

Table 1 Parameters of Ca^{2+} sparks in embryonic mammalian skeletal muscle

	$\Delta F/F_o$	FTHM (ms)	FWHM (μm)
E18 WT (n = 280 sparks, 129 cells)	1.6 ± 0.6	84.5 ± 46	3.5 ± 1.1
E18 RyR-1 null (n = 341 sparks, 67 cells)	1.3 ± 0.7*	44.9 ± 49*	2.7 ± 1.2*
E18 RyR-3 null (n = 412 sparks, 66 cells)	1.6 ± 0.6	43.2 ± 25*	2.6 ± 0.6*

*Asterisks indicate statistical significance $p < 0.05$ (*) in an unpaired t-test against the same parameter in E18 WT cells. Only peak $\Delta F/F_o$ of sparks in RyR-3 null cells was not significantly different from that of sparks in control (wt) cells.

The ability of caffeine to activate RyR-3 channels has been difficult to determine in situ. Caffeine-induced SR Ca^{2+} release assayed by a Ca^{2+} indicator in permeabilized limb muscle bundles was found to be depressed in RyR-1 null compared with wt embryonic muscle. (Takeshima et al., 1995). This study suggested RyR-3 channels were less sensitive to caffeine than RyR-1 channels. We now find through confocal Ca^{2+} imaging that caffeine is at least two orders of magnitude more efficacious in RyR-1 null muscle than in RyR-3 null muscle and, therefore, RyR-3 channels must be considerably more responsive to caffeine than RyR-1 channels. In amphibian skeletal muscle the main effect of submillimolar caffeine (0.5 mM) is to increase the peak spark fluorescence ~1.3-fold (Gonzalez et al., 1999). In RyR-1 null embryonic cells, similar to previous determinations in wt cells of the same age (Conklin et al., 1999a), we found that the main effect of caffeine (0.1 mM) was to increase the event duration ~1.9-fold. A mechanism involving the recruitment of additional channels by caffeine was proposed to explain the increase in peak fluorescence (Gonzalez et al., 1999). In our case, we suggest that caffeine increases the ability of channels already committed to the spark to reopen a second time following the initial opening and closing event that produces the spark. Reopening of channels would be expected to lengthen the decay phase of the spark without necessarily increasing the Ca^{2+} released at the peak. Reopenings could be driven by an increase in the Ca^{2+} sensitivity of RyR-3 channels, which we suggest might be due to enhanced channel phosphorylation rather than to a direct "nucleotide effect" of caffeine on the RyR (Coronado et al., 1994). Direct stimulatory effects of caffeine on the RyR occur at concentrations 10- to 50-fold larger than those reported here. Moreover, the phosphodiesterase inhibitor IBMX (3-isobutyl-1-methylxanthine) prolonged the time course of sparks in RyR-1 null cells much like submillimolar caffeine (not shown). Sequence comparisons have shown 21 potential phosphorylation sites, 3 of which are common to all RyRs, and 7 others are only found in the RyR-3 (Marziali et al., 1996). In addition, one potential cAMP-dependent phosphorylation site KRXXS/T is conserved in all RyR-3 splice variants (Marziali et al., 1996). Mutagenesis and expression analyses followed by Ca^{2+} spark determinations should provide additional information on the molecular basis of the high caffeine sensitivity of RyR-3.

This work was supported by National Institutes of Health Grants HL47053 and AR 46448 (to R.C.), an American Heart Association Wisconsin Affiliate Predoctoral Fellowship (to M.C.), and Telethon Grant 1151 (to V.S.).

REFERENCES

Barone, V., F. Bertocchini, R. Bottinelli, F. Protasi, P. D. Allen, C. Franzini-Armstrong, C. Reggiani, and V. Sorrentino. 1998. Contractile impairment and structural alterations of skeletal muscles from knock-out mice lacking type 1 and type 3 ryanodine receptors. *FEBS Lett.* 422: 160–164.

Bertocchini, F., C. E. Ovitt, A. Conti, V. Barone, H. R. Scholer, R. Bottinelli, C. Reggiani, and V. Sorrentino. 1997. Requirement for the ryanodine receptor type 3 for efficient contraction in neonatal skeletal muscles. *EMBO J.* 16:6956–6963.

Block, B. A., T. Imagawa, K. P. Campbell, and C. A. Franzini-Armstrong. 1988. Structural evidence for direct interaction between the molecular components of the transverse tubule/sarcoplasmic reticulum junction in skeletal muscle. *J. Cell Biol.* 107:2587–2600.

Carl, S. L., K. Felix, A. H. Caswell, N. R. Brandt, W. J. Ball, Jr., P. L. Vaghy, G. Meissner, and D. G. Ferguson. 1995. Immunolocalization of sarcolemmal dihydropyridine receptor and sarcoplasmic reticular triadin and ryanodine receptor in rabbit ventricle and atrium. *J. Cell Biol.* 129:673–682.

Chen, S. R. W., X. Li, K. Ebisawa, and L. Zhang. 1997. Functional characterization of the recombinant type 3 Ca^{2+} release channel (ryanodine receptor) expressed in HEK292 cells. *J. Biol. Chem.* 272: 24234–24246.

Cheng, H., W. J. Lederer, and M. B. Cannell. 1993. Calcium sparks: elementary events underlying excitation-contraction coupling in heart muscle. *Science.* 262:740–744.

Conklin, M. W., V. Barone, V. Sorrentino, and R. Coronado. 1999b. Contribution of ryanodine receptor type 3 to Ca^{2+} sparks in embryonic mouse skeletal muscle. *Biophys. J.* 77:1394–1403.

Conklin, M. W., P. Powers, R. G. Gregg, and R. Coronado. 1999a. Ca^{2+} sparks in embryonic mouse skeletal muscle selectively deficient in dihydropyridine receptor α1S or β1 subunits. *Biophys. J.* 76:657–669.

Conklin, M. W., H. Takeshima, V. Sorrentino, and R. Coronado. 1999c. Calcium sparks are produced independently by RyR-1 or RyR-3 in mouse embryonic myotubes. Biophysical Society Meeting, New Orleans, LA, February 12–16, 2000 (Abstract).

Coronado, R., J. Morrissette, M. Sukhareva, and D. M. Vaughan. 1994. Invited review: structure and function of ryanodine receptors. *Am. J. Physiol. (Cell Physiol.).* 35:C1485–C1504.

Flucher, B. E., A. Conti, H. Takeshima, and V. Sorrentino. 1999. Type 3 and type 1 ryanodine receptors are localized is triads of the same mammalian skeletal muscle fibers. *J. Cell Biol.* 146:621–629.

Franzini-Armstrong, C. 1991. Simultaneous maturation of transverse tubules and sarcoplasmic reticulum during muscle differentiation in the mouse. *Dev. Biol.* 146:353–363.

Gonzalez, A., N. Shirokova, W. G. Kirsch, and E. Rios. 1999. Voltage and caffeine increase Ca^{2+} spark amplitude in skeletal muscle. *Biophys. J.* 76:385*a.* (Abstr.).

Hakamata, Y., J. Nakai, H. Takeshima, and K. Imoto. 1992. Primary structure and distribution of a novel ryanodine receptor/calcium release channel from rabbit brain. *FEBS Lett.* 312:229–235.

Jeyakumar, L. H., J. A. Copello, A. M. O'Malley, G.-M. Wu, R. Grassucci, T. Wagenknecht, and S. Fleischer. 1998. Purification and characterization of ryanodine receptor 3 from mammalian tissue. *J. Biol. Chem.* 273:16011–16020.

Klein, M. G., H. Cheng, L. F. Santana, Y.-H. Jiang, W. J. Lederer, and M. F. Schneider. 1996. Two mechanisms of quantized calcium release in skeletal muscle. *Nature.* 379:455–458.

Marziali, G., D. Rossi, G. Giannini, A. Charsworth, and V. Sorrentino. 1996. cDNA reveals a tissue specific expression of alternatively spliced transcripts of the ryanodine receptor type 3 (RyR3) calcium release channel. *FEBS Lett.* 394:76–82.

Murayama, T., and Y. Ogawa. 1997. Characterization of type 3 ryanodine receptor (RyR3) of sarcoplasmic reticulum rabbit skeletal muscles. *J. Biol. Chem.* 272:24030–24037.

Nakai, J., T. Imagawa, Y. Hakamata, M. Shigekawa, H. Takeshima, and S. Numa. 1990. Primary structure and functional expression from cDNA of the cardiac ryanodine receptor/calcium release channel. *FEBS Letters* 272:169–177.

Nakai, J., R. T. Dirksen, H. T. Nguyen, I. N. Pessah, K. G. Beam, and P. D. Allen. 1996. Enhanced dihydropyridine receptor channel activity in the presence of ryanodine receptor. *Nature*. 380:72–75.

Nakai, J., T. Ogura, F. Protasi, C. Franzini-Armstrong, P. D. Allen, and K. G. Beam. 1997. Functional non-equality of the cardiac and skeletal ryanodine receptors. *Proc. Natl. Acad. Sci. USA.* 94:1019–1022.

Ottini, L., G. Marziali, A. Conti, A. Charlesworth, and V. Sorrentino. 1996. Alpha and beta isoforms of ryanodine receptors from chicken skeletal muscle are the homologues of mammalian RyR1 and RyR3. *Biochem. J.* 315:207–216.

Percival, A. L., A. J. Williams, J. K. Kenyon, M. M. Grinsell, J. A. Airey, and J. L. Sutko. 1994. Chicken skeletal muscle ryanodine receptor isoforms: ion channel properties. *Biophys. J.* 67:1834–1850.

Shacklock, P. S., W. G. Wier, and C. W. Balke. 1995. Local calcium transients (Ca^{2+} sparks) originate at transverse tubules in rat heart cells. *J. Physiol.* 487:601–608.

Shirokova, N., J. Garcia-Martinez, and E. Rios. 1998. Local calcium release in mammalian skeletal muscle. *J. Physiol.* 512:377–384.

Sonnleitner, A., A. Conti, F. Bertocchini, H. Schindler, and V. Sorrentino. 1998. Functional properties of the ryanodine receptor type 3 (RyR3) Ca^{2+} release channel. *EMBO J.* 17:2790–2798.

Sorrentino, V., and C. Reggiani. 1999. Expression of ryanodine receptor type 3 in skeletal muscle: a new partner in excitation-contraction coupling? *Trends Cardiovasc. Med.* 9:53–60.

Sutko, J. L., and J. A. Airey. 1996. Ryanodine receptor Ca^{2+} release channels: does diversity in form equals diversity in function? *Physiol. Rev.* 76:1027–1071.

Takekura, H., L. Bennett, T. Tanabe, K. G. Beam, and C. Franzini-Armstrong. 1994. Restoration of junctional tetrads in dysgenic myotubes by dihydropyridine receptor cDNA. *Biophys. J.* 67:793–803.

Takekura, H., M. Nishi, T. Noda, H. Takeshima, and C. Franzini-Armstrong. 1995. Abnormal junctions between surface membrane and sarcoplasmic reticulum in skeletal muscle with a mutation targeted to the ryanodine receptor. *Proc. Natl. Acad. Sci. USA.* 92:3381–3385.

Takeshima, H., T. Ikemoto, M. Nishi, N. Nishiyama, M. Shimuta, Y. Sugitani, J. Kuno, I. Saito, H. Saito, M. Endo, M. Iino, and T. Noda. 1996. Generation and characterization of mutant mice lacking ryanodine receptor type 3. *J. Biol. Chem.* 271:19649–19652.

Takeshima, H., I. Masamitsu, H. Takekura, M. Nishi, J. Kuno, O. Minowa, H. Takano, and T. Noda. 1994. Excitation-contraction uncoupling and muscular degeneration in mice lacking functional skeletal muscle ryanodine-receptor gene. *Nature.* 369:556–559.

Takeshima, H., S. Nishimura, T. Matsumoto, H. Ishida, K. Kangawa, N. Minamino, H. Matsuo, M. Ueda, M. Hanaoka, T. Hirose, and S. Numa. 1989. Primary structure and expression from complementary DNA of skeletal muscle ryanodine receptor. *Nature.* 339:439–445.

Takeshima, H., T. Yamazawa, T. Ikemoto, H. Takekura, M. Nishi, T. Noda, and M. Iino. 1995. Ca^{2+}-induced Ca^{2+} release in myocytes from dyspedic mice lacking the type 1 ryanodine receptor. *EMBO J.* 14: 2999–3006.

Tsugorka, A., E. Rios, and L. A. Blatter. 1995. Imaging elementary events of calcium release in skeletal muscle cells. *Science.* 269:1723–1726.

Ward, C., D. Castillo, F. Protasi, Y. Wang, S. Chen, M. Schneider, and P. Allen. 1999. Expression of RyR_3 but not RyR_1 produces Ca^{2+} sparks in dyspedic myotubes. *Biophys. J.* 76:368*a.* (Abstr.).

Yao, Y., J. Choi, and I. Parker. 1995. Quantal puffs of intracellular Ca^{2+} evoked by inositol trisphosphate in Xenopus oocytes. *J. Physiol.* 482: 533–553.